Chemotherapy-exacerbated cancer cell colonization of the lung is mediated by host-ATF3-dependent and -independent processes.

Justin Middleton[†]

Institutions: Molecular, Cellular and Developmental Biology Graduate Program, Department of Biological Chemistry and Pharmacology, College of Medicine.

Introduction

While chemotherapy (chemo) is currently a widely used therapy for the treatment of many cancers, there are limits to its effectiveness in certain types of cancer and at certain stages[1-4]. Much of this has been attributed to the intrinsic ability of cancer cells to resist treatment[5]. Recently, however, much work has been done in understanding how chemo affects non-cancer cells in the host, the organism carrying the cancer cells[6, 7]. Thus far, studies showed that many of the host-dependent effects of chemo are the result of changes to the immune system, in particular myeloid cells. Chemo has been shown to increase the abundance of immunosuppressive immature monocytes and pro-angiogenic $Tie2^{+}$ macrophages in tumors, both of which enhance cancer progression[8, 9]. MMP9 from macrophages is also implicated in participating in chemo-exacerbated colonization of the lung by cancer cells[10]. Other, non-immune host cells may be altered by chemo to promote metastasis as well, including endothelial cells (ECs) and fibroblasts, although these cells can also interact with the immune system through changes in cytokine production[11-13]. How chemo induces these changes is less well understood, although there are several possibilities, including the bias of hematopoietic progenitors toward myeloid production after chemo, increased formation of hypoxia-induced pre-metastatic niches, and systemic

[†] Other contributing authors: Jared Fehlman, College of Arts and Sciences, and Dr. Tsonwin Hai.

inflammation caused by the release of death-associated molecular patterns (DAMPs) from cells killed by treatment[13-16]. One overall concept that these possible causes fall under is chemo-induced stress, a phenomenon we have examined in our previous work on the stressed-induced gene, *ATF3*.

ATF3 is a member of the ATF/AP-1/CREB family of genes encoding transcription factors. The *ATF3* gene, in normal conditions, is expressed at low levels in most cells but upon insult or changes in homeostasis rapidly increases – in a manner not specific to either cell types or to stimuli[17, 18]. This non-specific reaction of the *ATF3* gene to stress, combined with the multitude of signaling pathways involved in ATF3 induction, led us to describe *ATF3* as a hub of cellular stress response[19]. Upon production, ATF3 protein can go on to regulate thousands of genes in a context- and cell-dependent manner, and plays an important role in regulating the inflammatory response. Using human breast cancer samples, we previously determined that high levels of ATF3 in mononuclear cells in tumor stroma – the non-cancer region of the tumor microenvironment – correlated with worse outcome. To test the functional importance of ATF3, we generated *ATF3* knockout (KO) mice and found that ATF3 in host cells (host-ATF3) is critical for cancer cells to metastasize from the primary tumor to the lung – the second site for the MVT-1 breast cancer model[20]. More recently, we discovered that adding the additional stress of chemo further increased metastasis to the lung, again in a host-ATF3-dependent manner[21]. Interestingly, in the primary tumor, we found an increase in the number of tumor microenviroments of metastasis (TMEMs), a microanatomical structure that allows the entry of cancer cells into the bloodstream, in wildtype (WT) mice treated with paclitaxel (PTX), but their KO counterparts. The increase in TMEMs corresponded to an increase in disseminated cancer cells (DCCs) in the bloodstream, suggesting a means for the observed increase in metastasis.

However, cancer cell escape from the primary tumor is only one step of metastasis, and many cells either fail to survive the transit to secondary sites or go dormant once there[22]. Cancer cells in secondary sites rarely flourish unless certain conditions are met, such as high levels of stress signaling or inflammation[23, 24]. Understanding how DCCs at the secondary site are affected by chemo is especially important in a clinical setting, where chemo is often used as an adjuvant therapy that takes place after the primary tumor is removed. Therefore, we decided to look further into the effects of ATF3 on cancer cell colonization of the lung.

Colonization can be roughly defined as starting when circulating cancer cells have arrested at a secondary site and ending when individual colonies begin growing to clinically detectable levels[25]. This process can last several days to years in humans. To colonize the lung, cancer cells need to accomplish several steps, including attachment to the vessel wall, extravasation into the lung parenchyma, avoiding death in a foreign environment and eventual growth into a metastatic nodule[26]. During colonization, early adhesion of cancer cells to ECs in the lining of blood vessels requires active interactions between cell adhesion molecules on the surface of ECs and cancer cells[27]. Then, tight junctions between ECs must then be disrupted in order for cancer cells to extravasate into the lung parenchyma, a process that involves not only intrinsic EC signaling, but also platelets and other immune cells[28, 29].

Among all of the immune cells, myeloid-lineage cells are the most documented as participating in colonization. Inflammatory monocytes (iMs) suppress natural killer (NK) cell cytotoxic activity; while metastasis associated macrophages (MAMs) – which are derived from iMs – assist in extravasation[30-32]. Neutrophils in the pre-metastatic niche promote the proliferation of metastasis initiating cells through the production of leukotrienes[33]. But overall, as opposed to the increasing number of reports about the effect of chemo on myeloid cells in primary tumors, little

is known about how myeloid cells at metastatic sites respond to the same chemo stress. In our previous work, we identified ATF3 in myeloid cells (myeloid-ATF3) as important for increasing the metastasis of cancer cells from primary tumors, but we have not established whether it plays a role in colonization[20]. As a result of this previous work, and the importance of myeloid cells in colonization, we decided to use an experimental metastasis model to test whether chemo-exacerbated colonization of the lung by breast cancer cells is dependent on myeloid-ATF3.

Methods

Animal studies

Age-matched (6-10 wk) FVB/N WT, *ATF3* KO, ATF3$^{f/f}$ and LysM-Cre/*ATF3*$^{f/f}$ mice were used for all experiments. For the experimental metastasis model, mice were intraperitoneally (IP) injected with either phosphate-buffered saline (PBS), 150 mg/kg body weight cyclophosphamide (CTX) (Cayman Pharmaceuticals) or 20 mg/kg paclitaxel (Sigma) in a 1:1:2 ratio of cremophor EL:ethanol:PBS (Sigma). Four days later, turbo green fluorescent protein (tGFP)-labeled MVT-1 breast cancer cells (1 x 10^6 cells in PBS) or tGFP-labeled Met-1 breast cancer cells (2x10^6 cells in PBS) were intravenously (IV) injected into the tail vein. Lungs were collected at the indicated time points. For perfusion assays, we adapted a previously used protocol[34]. Briefly, after mice from experimental metastasis experiments were sacrificed, the left atrium of the heart was cut and a 25 gauge needle attached to a length of tubing was inserted into the right ventricle. Mice were then perfused for 5 minutes with PBS using a peristaltic pump, and then lung were inflated and fixed with 10% formalin.

Immunofluorescence (IF) Microscopy

Staining was performed on formalin-fixed, paraffin-embedded tissue sections. Antibodies used were anti-tGFP (1:3000), anti-phospho-histone H3 (1:200), anti-cleaved caspase-3 (1:200). TOPRO3 was used as a counterstain. Images were captured on a Leica TCS SL confocal microscope (Leica Microsystems). For colony counting, at least eight fields of views (FOVs) were taken per lung. Image analysis was performed using FIJI after file names were randomized.

Cell culture and isolation

TurboGFP-MVT1 and Met-1 cells were cultured in DMEM supplemented with 10% FBS and 1% pen/strep. Mouse lung endothelial cells (mLECs) were isolated via a procedure adapted from several protocols[35, 36]. Briefly, lungs from 7-8 day old FVB/N pups were aseptically removed from and placed into Miltenyi C-tubes (Miltenyi Biotec) with 10 mL of a 1 mg/mL collagen and dispase solution and then minced into 2 mm^2 pieces. This mixture was then incubated at 37° C with constant agitation for 30 minutes, whereupon 75 ul of DNase was added, followed by 30 min more of incubation. The lungs were then pulverized using a gentleMACS Dissociator (Miltenyi Biotec). The resulting slurry was passed through a 100 um filter. After pelleting, the cells were mixed with CD31 magnetic beads as recommended (Miltenyi Biotec), and then passed through a magnetic column. The retained cells were then cultured on gelatin-coated plates with EndoGRO-LS complete media (EMD Millipore) with 1% pen-strep. Endothelial cell purity was tested via flow cytometry using a CD31 antibody.

Adhesion Assay

FVB/N WT mice were injected with PBS or CTX (150 mg/kg body weight). After 18 hours, mice were sacrificed and blood was collected via cardiac puncture, from which serum was isolated after clotting and centrifugation at 2000 x g. Serum from several mice of the same

groups were then mixed, and 15 ul of serum was then added to LECs in culture in a 12-well plate for 6 hours. LECs were then washed with PBS and cultured in normal media for 2 days, upon which time 10^5 MVT-1 cells labeled with CellTracker Green (Invitrogen) were added to the wells for 30 minutes. Unattached cells were washed away twice with PBS, and then cells were imaged using a Nikon Diaphot 300 microscope (Nikon). Experimental conditions were in triplicate and nine 100X images were captured per well. Image names were randomized and cells were counted using FIJI.

Flow Cytometry

Single cell suspensions from lungs were prepared and stained as previously described[20] using the antibodies listed in Table 1. Cells were analyzed on LSR II and Fortessa flow cytometers (BD Biosciences). Cell sorting was performed on an Aria III flow cytometer (BD), followed by post-sort analyses to test purity. Forward scatter and side scatter were used to exclude debris or aggregates, and unstained and single stained cells were used as gating controls.

Table 1: Antibodies

Target	Fluorophore	Company
CD11b	APC-cy7	eBioscience
F4/80	FITC	eBioscience
Ly6C	eF450	eBioscience
Ly6G	APC	eBioscience
VEGFR1	PE	R&D System
Lineage	FITC	eBioscience
Sca	APC	eBioscience
c-Kit	APC-cy7	eBioscience
CD34	eF450	eBioscience
CD64	PE	Miltenyi
IL7R	PE-cy7	eBioscience
tGFP	None	Invitrogen
CD31	PE	eBioscience
CD31	None	Abcam
p-H3	None	Cell
Cleaved caspase-3	None	Cell

Statistics

Unless otherwise noted, statistical methods were two-way ANOVA with a Holm-Šídák correction using SigmaPlot software. One-way ANOVA and Student t test (two-sided) were also

used as indicated in figure legends. Figures were generated using GraphPad Prism 6.0. Data represent the mean ± SEM; $P < 0.05$ was considered statistically significant.

Results

Chemotherapy increases cancer cell colonization in WT, but not ATF3 KO mice.

To examine the colonization of the lung by cancer cells, we used an experimental metastasis model where tGFP-labeled MVT-1 breast cancer cells were IV injected into the tail vein of WT or KO mice (Fig. 1A, time point 0 day). We observed colony formation in the lung up to 72 hours post-injection. This time frame allows us to examine the earliest stages of colonization when cancer cells arrest at the lungs and cross into the parenchyma in a process known as seeding. To test the effect of chemo on colonization, four days prior to the IV injection, we treated the mice with CTX which, based on pharmacokinetics, would largely be eliminated from the body in 24 hours[37]. By waiting to inject cancer cells until after that time, we allow no opportunity for the chemo to have any direct effect on cancer cells, letting us monitor the effects of the drugs on the host. Three day post-cancer cell injection, we isolated the lungs, and detected cancer cells by IF analysis using a tGFP antibody. We identified an increase in the number of colonies in the lungs of WT mice following CTX treatment, but no increase in KO mice (Fig. 1B, 1C). This effect was also present in mice injected with Met-1 cells (data not shown), which have different oncogenic events, and in mice injected with PTX (data not shown), a drug with entirely different mechanisms of action than CTX. The reproducibility

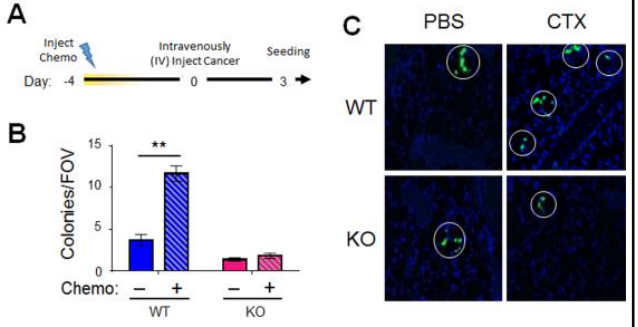

Fig. 1: A. Experimental metastasis model. B. Lung colony number per FOV (at least 8 FOVs). C. Representative images of all four groups. Green = cancer cells, Blue = DNA (TOPRO3), White circles = colonies. (n = 3-9) ** = $p < .01$.

of this phenotype with different chemo drugs and cancer cells indicates that it is not an artifact of a specific experimental setup, but likely a broader phenomenon.

We also noticed that at 72 hours there was a significant difference in size of these colonies (Fig. 2B). In general, the colonies of WT-treated mice were roughly 40-50% larger than those of the other groups, suggesting that the rate of colony growth was larger in this group than any other. This could be due to increases in proliferation or decreases in cell death, or both. Overall, these data indicate that WT-treated mice have the most favorable environment for colonization and cancer cell growth.

A colonization time-course assay reveals ATF3-dependent and ATF3-independent processes.

Based on this result, we set out to determine what processes of colonization were affected by chemo. We therefore analyzed the lungs at various time points using the experimental metastasis model combined with CTX pre-treatment. Curiously, we found a switch-point in our phenotype. Before 18 hours, the number of colonies in the lung was increased by CTX in an ATF3-independent manner, while after 18 hours the colony increase was dependent on host-*ATF3* (Fig. 2A). We therefore surmised that at least two different processes were affected by chemo. Conceptually, colonization can be divided into 4 processes: cancer cell adhesion to blood vessels

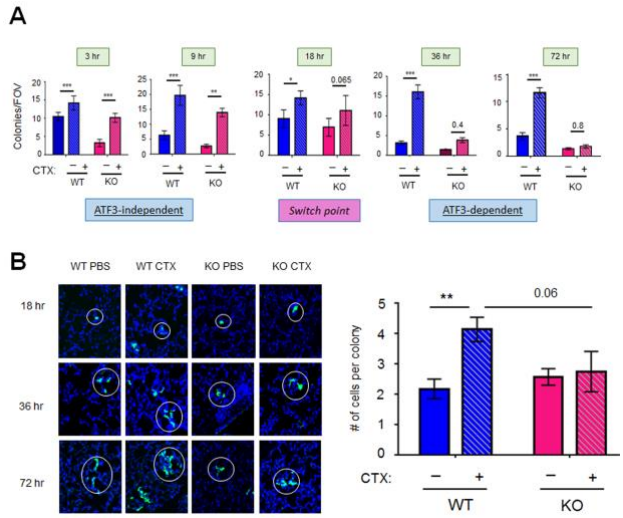

Fig. 2: A. Time course assay. B. (Left) Representative images of colony sizes over time. White circles indicate one colony. (Right) Number of cells per colony at 72 hours. Green = cancer cells, Blue = DNA (TOPRO3), White circles = colonies. (n = 3-9) * = p < .05, ** = p < .01, *** = p < .001.

in the initial phases, followed by extravasation into the lung parenchyma, and finally growth, a net result of two biological processes (proliferation and death). Interestingly, some researchers have documented the time at which different processes occur in the experimental metastasis model using live imaging of the lung[30]. That literature indicates that cancer cells do not extravasate until roughly 12 hour post-arrest, meaning that the early, *ATF3*-independent increases in colnization are likely due to increases in adhesion, while the later, *ATF3*-dependent chemo-exacerbated colonization may be due to an increase in extravasation and growth.

CTX increases the adhesiveness of mLECs and levels of N-cadherin.

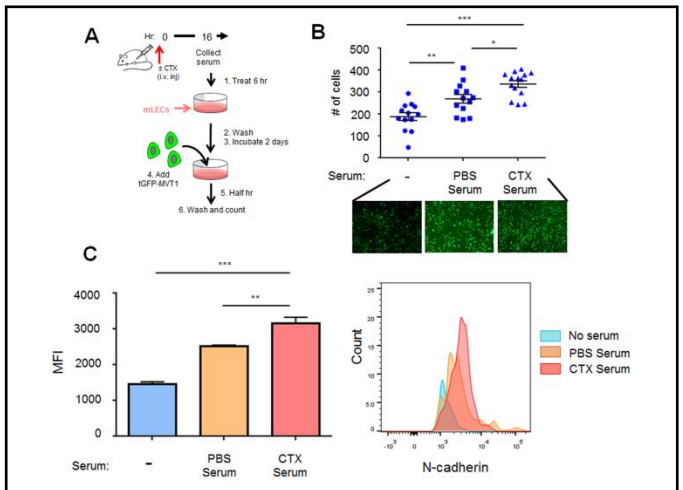

Fig. 3: A. In vitro adhesion model. B. Average number of cells per FOV (n = 13). C. (Left) MFI of N-cadherin among mLECs treated with indicated serum. (Right) Representative histogram. (n = 3) * = $p < .05$, ** = $p < .01$, *** = $p < .001$.

Before cancer cells are able to exit the bloodstream and colonize the lung, they must adhere to the surface of the blood vessel via cell adhesion molecules. As such, we proposed the early, *ATF3*-independent time points as likely being the result of differences in cancer cell adhesion to the ECs of the blood vessel. Because of the difficulty of ascertaining differences in adhesion in vivo, we decided to test the effect of CTX on adhesion in vitro. Since CTX is a pro-drug that needs to be metabolized to produce active products, we collected the serum of mice treated with CTX 18 hours after injection, or with PBS as a control. We used this PBS- or CTX-serum to treat mLEC monolayers, followed by washing and the addition of CellTracker Green-labeled cancer cells as schematized in Fig. 3A. At 30 minutes after cancer cell addition, we quantified the adherent cells

after removing non-adherent cells by washing. As shown in Fig. 3B, serum from PBS-treated mice markedly enhanced adhesion, a result that is not surprising based on the likely presence of soluble factors in normal serum that promote EC adhesiveness. Interestingly, we noticed a stepwise increase when ECs were treated with CTX-serum that was significantly different that ECs treated with PBS-serum. This could be the result of active CTX metabolites present in the serum or changes in the composition of soluble factors in serum, or both. In any case, this data indicates that CTX promotes the adhesiveness of ECs. Increasing the number of cell adhesion molecules on the surface of ECs is a key mechanism to enhance the interactions of ECs with other cells[27]. To explore this mechanistically, we screened several possible candidates for cell adhesion molecules on ECs known to interact with cancer cells. We determined the levels of cell adhesion molecules on mLECs after serum treatment through IF staining followed by flow cytometry. We found no changes in E-selectin (data not shown), a widely documented mediator of EC-cancer cell interactions[38, 39]. However, we found a statistically significant, stepwise increase in the median fluorescence intensity (MFI) of N-cadherin on ECs (Fig. 3C) that corresponded to the increases in adhesion we observed previously (Fig. 3B). N-cadherin is a cell adhesion molecule present on both cancer cells and ECs that has drawn increasing attention for its role in promoting cancer cell adhesion and extravasation[40-42]. In light of this literature, the correlation between adhesion and N-cadherin levels on the surface of mLECs suggests that N-cadherin may be a mediator of CTX-induced increases in adhesion.

Extravasation and cancer cell death may play a role in chemo-exacerbated colonization.

For the ATF3-dependent time points (18 hours post-cancer cell injection and afterward), we tested extravasation, cell death and proliferation. This is because they were shown to occur at 12-36 hours post-cancer cell injection, which largely overlaps with the time points of interest in this

project. In order to test extravasation, we adapted a perfusion-based assay in which mice were IV injected with cancer cells and their lungs were then perfused with saline through the right ventricle of the heart to remove cancer cells in the lung that had not exited the blood stream. Any cancer cells that remained after perfusion represent cells that have already extravasated and entered the lung parenchyma. Control perfusions performed at 30 minutes post-injection – a time in which little extravasation could have occurred – showed 75% decrease in cells, while perfusions performed at 72 hours – when the vast majority of cells should be extravasated – showed no change in the amount of cells (Fig. 4A). Using high magnification IF, we also observed the majority of cancer cells present in perfused lungs were indeed outside of blood vessels (Fig. 4B). Perfusions performed at the switch point (18 hrs) revealed that cancer cells in CTX-treated WT mice were completely resistant to perfusion, while cells in CTX-treated KO mice were only partially resistant (Fig. 4C). This difference suggests that extravasation could explain, at least partially, the higher number of colonies in the CTX treated WT lung than that in the corresponding KO lung (Fig. 2A)

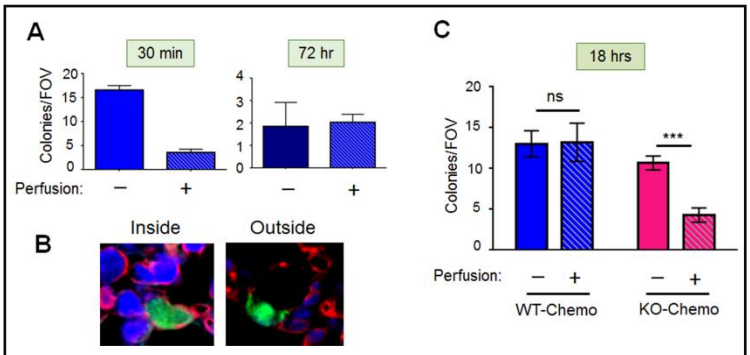

Fig. 4: A. WT mice were injected with cancer cells and analyzed at 30 min or 72 hr post-injection with (+) or without (-) perfusion immediately before collecting the lungs. B. Representative high magnification (630X) images of cancer cells inside and outside blood vessels. Green = cancer cells, Red = CD31, Blue = DNA (TOPRO3). C. Colonies per FOV in WT-Chemo and KO-Chemo groups with or without perfusion. (n = 9-17) *** = p < .001.

In addition to extravasation, increased levels of cancer cell proliferation could explain the observed increase in colonies in the WT-treated group. Phospho-histone H3 (p-H3) is an accepted marker for delineating proliferating cells[43]; therefore we used antibodies against p-H3 and tGFP on lungs from 18 hours to determine if there were differences in the number of

proliferating cancer cells. The number of p-H3^{+} tGFP^{+} cells was largely unchanged at this time point (Fig. 5A). These results indicate that proliferation may not contribute to the observed differences in colony number or size, although more time points should be tested.

When we looked at cancer cell apoptosis at 18 hours using antibodies against activated caspase-3 (C3*), we observed a significant increase in dying cancer cells in KO animals (Fig. 5B). This effect appears to be genotype-based, and unaffected by CTX. When we combine the adhesion data with the results of the perfusion and C3* assays, we can generate an overall picture of the difference between WT-treated and KO-treated groups. While chemo increases the adhesion of cancer cells to mLECs, cancer cells in WT-treated mice extravasate at a significantly higher rate than those in KO-treated mice. The cells that do manage to extravasate in the KO mice are then subject to a three-fold increase in cell death, resulting in an overall decreased ability to colonize the lung by 72 hrs.

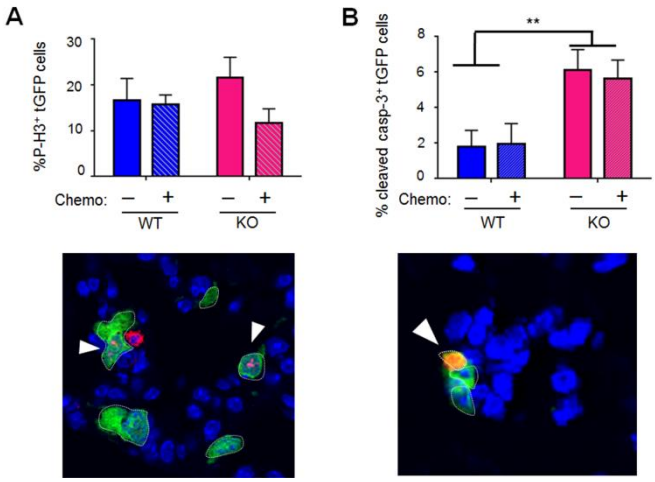

Fig. 5: A. (Top) Percent of tGFP cells positive for p-H3. (Bottom) Representative image. Dashed line = cancer cells. Arrowhead = p-H3 positive cancer cell. (n = 3-5) B. (Top) Percent of tGFP cells positive for C3*. (Bottom) Representative image. Dashed line = cancer cells. Arrowhead = c-C3 positive cancer cell. Green = cancer cells, Red = p-H3/C3*, Blue = DNA (TOPRO3). (n =4-7) ** = $p < .01$.

Myeloid cell abundance correlates with cancer colonization.

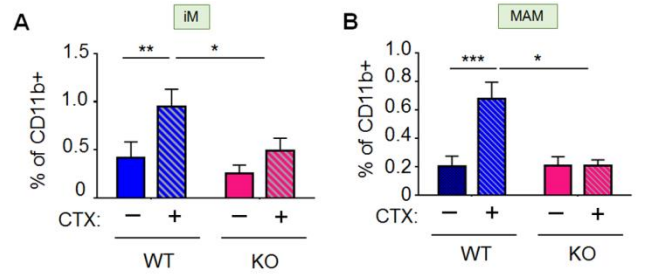

Fig. 6: A. Levels of iMs (CD11b^{+} F4/80^{+} Ly6C^{+}) and B. MAMs (CD11b^{+} F4/80^{+} Ly6C^{-} Ly6G^{-} VEGFR1^{+}) in the lung 18 hours after cancer cell injection. (n = 5-7) * = p < .05, ** = p < .01, *** = p < .001.

Previously, we showed that ATF3 in myeloid cells is important for the ability of myeloid cells to enhance metastasis. Since myeloid cells play an important role in the colonization process, we asked whether myeloid cells play a role in the chemo-exacerbation phenotype. At the 18 hour time point, we found an increase in iMs and MAMs in the lungs of CTX-treated WT mice compared to all other groups (Fig. 6A, 6B). Both of these cell types are immunosuppressive, and thus protect cancer cells from cytotoxic lymphocytes like CD8 T-cells and NK cells. MAMs have also been implicated in promoting cancer cell extravasation. Interestingly, the level of these myeloid subsets at 18 hours matches the colonization phenotype at 72 hours. This correlation led us to hypothesize that the abundance of these immune cells in the lungs has an impact on the levels of cancer cell colonization. As myeloid cells are hematopoietic cells, they are derived from progenitors in the bone marrow that must differentiate and then travel to the lung. Therefore, we decided to test whether ATF3 and CTX modulate the levels of progenitor cells in the bone marrow.

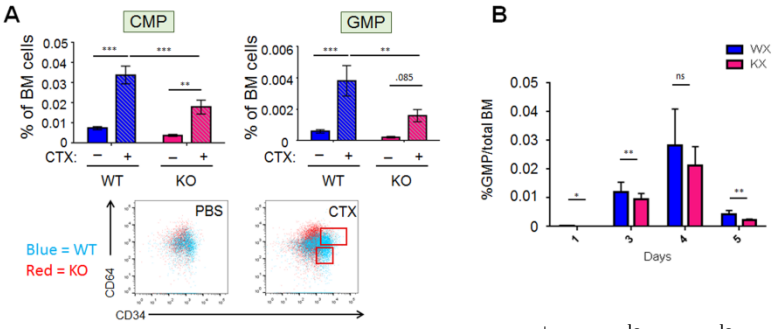

Fig. 7: A. (Top) Levels of CMPs (Lin^{-} Sca^{-} c-Kit^{+} CD64^{lo} CD34^{lo}) and GMPs (Lin^{-} Sca^{-} c-Kit^{+} CD64^{hi} CD34^{hi}) in the bone marrow five days after CTX injection. (Bottom) Representative flow diagrams of all four groups. (n =8-10) B. GMPs as a percentage of total bone marrow on the indicated days. (n = 4-10) * = p < .05, ** = p < .01, *** = p < .001.

Many chemo drugs, including cyclophosphamide, depopulate the bone marrow of hematopoietic cells, causing severe immune dysfunction[44]. This mass cell loss has been shown to be followed by a rebound that overshoots baseline levels of immune cells, and a shift in the myeloid-to-lymphoid cell ratio that favors myeloid cells[14, 45, 46]. As such, we wondered if this effect could explain the increase in certain myeloid subsets we observed at the 18 hour switch point. Both iMs and MAMs are derived from myeloid precursors, including the common myeloid progenitors (CMPs) and granulocyte-monocyte progenitors (GMPs) [47, 48]. We found that both CMPs and GMPs were increased as a percentage of bone marrow in CTX-treated mice compared to PBS-treated mice. Interestingly, the GMPs and CMPs in KO animals rebound significantly less than those in WT animals (Fig. 7A). It is important to note that these differences were detected at five days post-chemo injection, which is roughly equivalent to 18 hours post-cancer cell injection in our experimental metastasis model. Thus, at around the time when chemo-exacerbated colonization becomes ATF3-dependent, KO mice have less myeloid cells to be recruited from the bone marrow. For GMPs, this differential started at one day post-injection, and was largely maintained in the following days (Fig. 7B). These data suggest that there is a larger pool of myeloid precursors in the CTX-treated WT mice that can be mobilized during the inflammatory response triggered by cancer cell colonization.

Conditional KO of ATF3 in myeloid cells has a modest impact on colonization.

In order to definitively test whether *ATF3* in myeloid cells contributes to the chemo-exacerbation phenotype, we used a conditional KO model in which ATF3 is selectively deleted in myeloid cells by Cre-lox technology[49]. Using this model we found a small decrease in the number of colonies present in CTX-treated CKO (CKO-CTX) mice compared to CTX-treated flox/flox mice (f/f-CTX) (Fig. 8A). We also saw a small decrease in the average size of the colonies in CKO-CTX mice. Together, this decreased colony number and size led to a significant overall decrease in the cancer cell burden of CKO-CTX group compared to its counterpart (Fig. 8B). The results from the CKO are much less robust than the total KO, which may be due to myeloid-ATF3 playing a relatively small role in chemo-exacerbated colonization. However, there are some possible caveats we explore in our discussion.

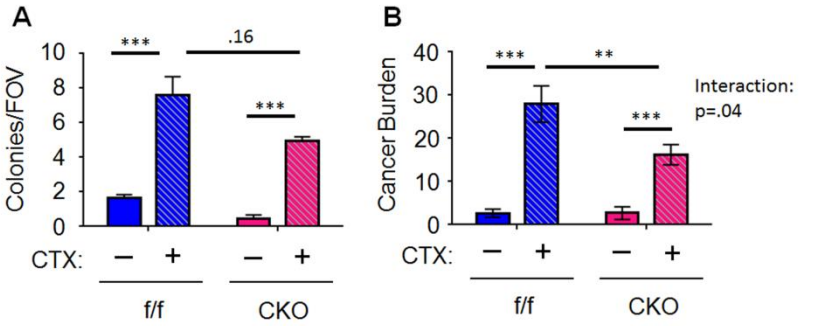

Fig. 8: A. Colonies per FOV and B. number of cells per FOV in treated and untreated ATF3 f/f mice and CKO mice. At least 8 FOVs per mouse. (n = 8-13) * = p < .05, ** = p < .01, *** = p < .001.

Discussion

Here we describe the effect of chemo on enhancing cancer cell colonization of the lung, and the contribution of the stress-gene, *ATF3*, to that process. Several important advances are presented in this work. (i) Chemo modulates at least two processes involved in cancer cell colonization: cell adhesion and extravasation. (ii) ATF3 promotes a more favorable environment for cancer cell to avoid death in the metastatic lung. (iii) ATF3 enhances the rebound of myeloid precursors and also contributes to a parallel increase of immunosuppressive myeloid subsets in the lung.

It should be noted that, as of now, these data together are largely correlative. While the stepwise increase in adhesion and N-cadherin levels treated with PBS-serum and CTX-serum is intriguing, and N-cadherin protein expression is known to be induced by chemo[50], more tests need to be done to establish if there is a causative relationship. Using N-cadherin blocking antibodies on mLEC monolayers in adhesion experiments will allow us to determine whether N-cadherin is responsible for increases in cancer cell adhesion, and to what extent. The question of what factor in the serum is causing the increase in adhesion may be quite challenging, based on the sheer number of possible candidates; however protein arrays for inflammatory cytokines and growth factors may help in narrowing down the potential culprits.

When we consider the ATF3-dependent aspects of chemo-exacerbated colonization, there is still the question of whether the differences in extravasation and cell death are linked to myeloid cells. Although we see increases in iMs and MAMs in the lung, we do not know if those cells in particular are causing the changes in cell death and extravasation. Testing those two processes in CKO mice will be one of our next steps. However, as mentioned previously, the CKO model produced relatively modest results compared to the total body KO. It is possible that the CKO mice used in this project are not the correct model for testing the importance of *ATF3* in myeloid cells. We propose several possible reasons for this ineffectiveness. (i) The CKO model depletes *ATF3* primarily in phagocytotic cells expressing LysM, which may not be present in the particular myeloid subsets we hypothesize are contributing to our phenotype. (ii) If *ATF3* is important in the production or mobilization of myeloid progenitors (see Fig. 7A), our CKO model is unlikely to produce major differences as LysM-Cre is only produced in a small fraction of progenitor cells (10%) [51, 52]. (iii) ATF3 in myeloid cells is important but redundancies exist, masking the impact of the deletion. For example, MMP9 is suggested to play a role in the

colonization of the lung by cancer cells, and is a gene upregulated by ATF3[20]. Though usually thought to be produced by myeloid cells, MMP9 can also be produced by ECs[53, 54]. Compensatory MMP9 production from ECs in the CKO model could theoretically make up for the absence of MMP9 produced by myeloid cells. In order to circumvent these possibilities, we plan to use clodronate liposomes, which eliminate monocytes and macrophages[30], with the goal of detecting whether these myeloid cells are necessary for chemo to exacerbate cancer cell colonization.

Of course, myeloid-*ATF3* may ultimately not be the most important source of ATF3 for this phenotype. In that case, there are multiple candidates for other cells in which *ATF3* may be important, but the most likely are ECs. Extravasation requires the breaking of tight junctions between ECs, a process that involves active processes within cells that may be regulated by ATF3. Factors released by ECs can also support cancer cell survival and proliferation. Therefore, in the near future we plan to cross floxed *ATF3* mice with Cdh5-Cre mice to generate an EC-selective KO[55]. To test for the possibility of redundancy between cell types, we will cross Cdh5-Cre and LysM-Cre mice and repeat the experiments displayed in Fig. 8.

We have identified extravasation and cell death as being markedly different between our WT-treated and KO-treated groups, and have proposed two myeloid subsets as being the potential mechanism for these changes. Performing in vitro assays to examine functional differences in these cells would provide more insight into whether these cells are involved. However, obtaining these cells in the number we need and within a reasonable amount of time will likely be difficult based on their low abundance in the lung. As such we will likely need to perform in vitro assays with the entire myeloid lineage of cells ($CD11b^+$ cells), rather than subsets, isolated from the lung or bone marrow-derived macrophages (BMDMs) as a proxy. Allowing for that, we plan to

use at least two assays in the future. (i) An in vitro extravasation assay that tests transendothelial migration of cancer cells through mLECs in a Boyden chamber with WT or KO BMDM treated with PBS-serum or CTX-serum in the bottom well. We would expect a greater amount of transendothelial migration in wells that include WT BMDM treated with CTX-serum. (ii) An in vitro NK cytotoxicity assay, in which cancer cells are labeled with a dye and then co-cultured with NK cells. By measuring the amount of released dye in the media, we can determine the levels of cancer cell death. We can then add myeloid cells isolated from each of our four groups and test whether the amount of cell death changes. Since we hypothesize that myeloid cells are suppressing the cytotoxic activity of NK cells in WT mice, we expect a decrease in cell death and co-cultures including WT myeloid cells.

In conclusion, CTX exacerbates colonization of the lung by cancer cells, in both host-ATF3-dependent and -independent manners, likely through a combination of effects, including adhesion, extravasation and the prevention of cell death. Understanding the molecular mechanisms of these changes, and the cellular causes of them, could help improve the outcomes of patients treated with chemo.

References

1. Morgan, G., Ward, R. & Barton, M. The contribution of cytotoxic chemotherapy to 5-year survival in adult malignancies. Clin Oncol. **16**, 549-560 (2004). https://www.ncbi.nlm.nih.gov/pubmed/15630849
2. Kim, H.A., Seong, M.K., Kim, E.K., Kang, E., Park, S., Hur, M.H., Song, B.J., Noh, W.C. & Korea Breast Cancer, S. Evaluation of the survival benefit of different chemotherapy regimens in patients with t1-2n0 triple-negative breast cancer. J Breast Cancer. **18**, 271-278 (2015). https://www.ncbi.nlm.nih.gov/pubmed/26472978
3. Rossi, L., Stevens, D., Pierga, J.Y., Lerebours, F., Reyal, F., Robain, M., Asselain, B. & Rouzier, R. Impact of adjuvant chemotherapy on breast cancer survival: A real-world

population. PLoS One. **10**, e0132853 (2015). https://www.ncbi.nlm.nih.gov/pubmed/26214853
4. Early Breast Cancer Trialists' Collaborative, G., Peto, R., Davies, C., Godwin, J., Gray, R., Pan, H.C., Clarke, M., Cutter, D., Darby, S., McGale, P., Taylor, C., Wang, Y.C., Bergh, J., Di Leo, A., Albain, K., Swain, S., Piccart, M. & Pritchard, K. Comparisons between different polychemotherapy regimens for early breast cancer: Meta-analyses of long-term outcome among 100,000 women in 123 randomised trials. Lancet. **379**, 432-444 (2012). https://www.ncbi.nlm.nih.gov/pubmed/22152853
5. Gonzalez-Angulo, A.M., Morales-Vasquez, F. & Hortobagyi, G.N. Overview of resistance to systemic therapy in patients with breast cancer. Adv Exp Med Biol. **608**, 1-22 (2007). https://www.ncbi.nlm.nih.gov/pubmed/17993229
6. Shree, T., Olson, O.C., Elie, B.T., Kester, J.C., Garfall, A.L., Simpson, K., Bell-McGuinn, K.M., Zabor, E.C., Brogi, E. & Joyce, J.A. Macrophages and cathepsin proteases blunt chemotherapeutic response in breast cancer. Genes Dev. **25**, 2465-2479 (2011). http://www.ncbi.nlm.nih.gov/pubmed/22156207
7. DeNardo, D.G., Brennan, D.J., Rexhepaj, E., Ruffell, B., Shiao, S.L., Madden, S.F., Gallagher, W.M., Wadhwani, N., Keil, S.D., Junaid, S.A., Rugo, H.S., Hwang, E.S., Jirstrom, K., West, B.L. & Coussens, L.M. Leukocyte complexity predicts breast cancer survival and functionally regulates response to chemotherapy. Cancer Discov. **1**, 54-67 (2011). http://www.ncbi.nlm.nih.gov/pubmed/22039576
8. Ding, Z.C., Lu, X., Yu, M., Lemos, H., Huang, L., Chandler, P., Liu, K., Walters, M., Krasinski, A., Mack, M., Blazar, B.R., Mellor, A.L., Munn, D.H. & Zhou, G. Immunosuppressive myeloid cells induced by chemotherapy attenuate antitumor cd4+ t-cell responses through the pd-1-pd-l1 axis. Cancer Res. **74**, 3441-3453 (2014). http://www.ncbi.nlm.nih.gov/pubmed/24780756
9. Chen, L., Li, J., Wang, F., Dai, C., Wu, F., Liu, X., Li, T., Glauben, R., Zhang, Y., Nie, G., He, Y., Qin, Z. Tie2 expression on macrophages is required for blood vessel reconstruction and tumor relapse after chemotherapy. Cancer Res. 76, 6828-6838 (2016). https://www.ncbi.nlm.nih.gov/pubmed/27758887
10. Gingis-Velitski, S., Loven, D., Benayoun, L., Munster, M., Bril, R., Voloshin, T., Alishekevitz, D., Bertolini, F. & Shaked, Y. Host response to short-term, single-agent chemotherapy induces matrix metalloproteinase-9 expression and accelerates metastasis in mice. Cancer Res. **71**, 6986-6996 (2011). http://www.ncbi.nlm.nih.gov/pubmed/21978934
11. Daenen, L.G., Roodhart, J.M., van Amersfoort, M., Dehnad, M., Roessingh, W., Ulfman, L.H., Derksen, P.W. & Voest, E.E. Chemotherapy enhances metastasis formation via vegfr-1-expressing endothelial cells. Cancer Res. **71**, 6976-6985 (2011). https://www.ncbi.nlm.nih.gov/pubmed/21975929
12. Tommelein, J., De Vlieghere, E., Verset, L., Melsens, E., Leenders, J., Descamps, B., Debucquoy, A., Vanhove, C., Pauwels, P., Gespach, C. P., Vral, A., De Boeck, A., Haustermans, K., de Tullio, P., Ceelen, W., Demetter, P., Boterberg, T., Bracke, M., De Wever, O. Radiotherapy-activated cancer-associated fibroblasts promote tumor

progression through paracrine igf1r activation. Cancer Res. **78**, 659-70 (2018). https://www.ncbi.nlm.nih.gov/pubmed/29217764
13. Balkwill, F. Cancer and the chemokine network. Nat Rev Cancer. **4**, 540–50 (2004). https://www.ncbi.nlm.nih.gov/pubmed/15229479
14. Cheng C., Adams, G. B., Perin, L., Wei, M., Zhou, X., Lam, B. S., Da Sacco, S., Mirisola, M., Quinn, D. I., Dorff, T. B., Kopchick, J. J., Longo, V. D. Prolonged fasting reduces IGF-1/PKA to promote hematopoietic stem cell-based regeneration and reverse immunosuppression. Cell Stem Cell. **14**, 810-823 (2014). https://www.ncbi.nlm.nih.gov/pubmed/24905167
15. Vyas, D., Laput, G. & Vyas, A. K. Chemotherapy-enhanced inflammation may lead to the failure of therapy and metastasis. Onco Targets Ther. **7**, 1015–1023 (2014). https://www.ncbi.nlm.nih.gov/pubmed/24959088
16. Hernandez, C., Huebener, P., & Schwabe, R. F. Damage-associated molecular patterns in cancer: a double-edged sword. Oncogene. **35**, 5931–5941 (2016). https://www.ncbi.nlm.nih.gov/pubmed/27086930
17. Hai, T. & Hartman, M.G. The molecular biology and nomenclature of the atf/creb family of transcription factors: Atf proteins and homeostasis. Gene. **273**, 1-11 (2001). https://www.ncbi.nlm.nih.gov/pubmed/11483355
18. Hai, T., Wolfgang, C.D., Marsee, D.K., Allen, A.E. & Sivaprasad, U. Atf3 and stress responses. Gene Expr. **7**, 321-335 (1999). https://www.ncbi.nlm.nih.gov/pmc/articles/PMC6174666/
19. Hai, T., Wolford, C.C. & Chang, Y.S. Atf3, a hub of the cellular adaptive-response network, in the pathogenesis of diseases: Is modulation of inflammation a unifying component? Gene Expr. **15**, 1-11 (2010). https://www.ncbi.nlm.nih.gov/pubmed/21061913
20. Wolford, C. C., McConoughey, S. J., Jalgaonkar, S. P., Leon, M., Merchant, A. S., Dominick, J. L., Yin, X., Chang, Y., Zmuda, E. J., O'Toole, S. A., Millar, E. K. A., Roller, S. L., Shapiro, C. L., Ostrowski, M. C., Sutherland, R. L., Hai, T. Transcription factor ATF3 links host adaptive response to breast cancer metastasis. J Clin Invest. **123**, 2893–2906 (2013). https://www.ncbi.nlm.nih.gov/pmc/articles/PMC3696548/
21. Chang, Y.S., Jalgaonkar, S.P., Middleton, J.D. & Hai, T. Stress-inducible gene atf3 in the noncancer host cells contributes to chemotherapy-exacerbated breast cancer metastasis. Proc Natl Acad Sci USA. **114**, E7159-E7168 (2017). https://www.ncbi.nlm.nih.gov/pubmed/28784776
22. Yeh, A. C., & Ramaswamy, S. Mechanisms of cancer cell dormancy--another hallmark of cancer? Cancer Res. **75**, 5014-5022 (2015). https://www.ncbi.nlm.nih.gov/pubmed/26354021
23. Linde, N., Fluegen, G., & Aguirre-Ghiso, J. A. The relationship between dormant cancer cells and their microenvironment. Adv Cancer Res. **132**, 45–71 (2016). https://www.ncbi.nlm.nih.gov/pmc/articles/PMC5342905/
24. Albrengues, J., Shields, M. A., Ng, D., Park, C. G., Ambrico, A., Poindexter, M. E., Upadhyay, P., Uyeminami, D. L., A. Pommier, V. Küttner, E. Bružas, L. Maiorino, C. Bautista, E. M. Carmona, P. A. Gimotty, D. T. Fearon, K. Chang, S. K. Lyons, K. E. Pinkerton, L. C. Trotman, M. S. Goldberg, J. T. Yeh, and M. Egeblad. Neutrophil

extracellular traps produced during inflammation awaken dormant cancer cells in mice. Science. **361**, eaao4227 (2018). https://www.ncbi.nlm.nih.gov/pubmed/30262472
25. Shibue, T. & Weinberg, R. A. Metastastic colonization: settlement, adaptation and propagation of tumor cells in a foreign tissue environment. Semin Cancer Biol. **21**, 99-106 (2011). https://www.ncbi.nlm.nih.gov/pubmed/21145969
26. Massagué, J., & Obenauf, A. C. Metastatic colonization by circulating tumour cells. Nature. **529**, 298–306 (2016). https://www.ncbi.nlm.nih.gov/pubmed/26791720
27. Bendas, G. & Borsig, L. Cancer cell adhesion and metastasis: selectins, integrins, and the inhibitory potential of heparins. Int J Cell Bio. **2012**, 676731 (2012). https://www.ncbi.nlm.nih.gov/pubmed/22505933
28. Reymond, N., d'Agua, B. B., Ridley, A. J. Crossing the endothelial barrier during metastasis. Nat Rev Cancer. **13**, 858-870 (2013). https://www.ncbi.nlm.nih.gov/pubmed/24263189
29. Strilic, B., Offermanns, S. Intravascular survival and extravasation of tumor cells. Cancer Cell. **32**, 282-293 (2017). https://www.ncbi.nlm.nih.gov/pubmed/28898694
30. Qian, B., Deng, Y., Im, J.H., Muschel, R.J., Zou, Y., Li, J., Lang, R.A. & Pollard, J.W. A distinct macrophage population mediates metastatic breast cancer cell extravasation, establishment and growth. PLoS One. **4**, e6562 (2009). http://www.ncbi.nlm.nih.gov/pubmed/19668347
31. Qian, B.Z., Li, J., Zhang, H., Kitamura, T., Zhang, J., Campion, L.R., Kaiser, E.A., Snyder, L.A. & Pollard, J.W. Ccl2 recruits inflammatory monocytes to facilitate breast-tumour metastasis. Nature. **475**, 222-225 (2011). http://www.ncbi.nlm.nih.gov/entrez/query.fcgi?cmd=Retrieve&db=PubMed&dopt=Citation&list_uids=21654748
32. Kitamura, T., Doughty-Shenton, D., Cassetta, L., Fragkogianni, S., Brownlie, D., Kato, Y., Carragher, N., Pollard, J. W. Monocytes differentiate to immune suppressive precursors of metastasis-associated macrophages in mouse models of metastatic breast cancer. Front Immunol. **8**, 2004 (2018). https://www.ncbi.nlm.nih.gov/pubmed/29387063
33. Wculek, S.K. & Malanchi, I. Neutrophils support lung colonization of metastasis-initiating breast cancer cells. Nature. **528**, 413-417 (2015). https://www.ncbi.nlm.nih.gov/pubmed/26649828
34. Lefrançais, E., Ortiz-Muñoz, G., Caudrillier, A., Mallavia, B., Liu, F., Sayah, D. M., Thornton, E. E., Headley, M. B., David, D., Coughlin, S. R., Krummel, M. F., Leavitt, A. D., Passegue, E., Looney, M. R. The lung is a site of platelet biogenesis and a reservoir for haematopoietic progenitors. Nature. **544**, 105–109 (2017). https://www.ncbi.nlm.nih.gov/pubmed/28329764
35. Sobczak, M., Dargatz, J., & Chrzanowska-Wodnicka, M. Isolation and culture of pulmonary endothelial cells from neonatal mice. J Vis Exp. **46**, 2316 (2010). https://www.ncbi.nlm.nih.gov/pubmed/21178973
36. Fehrenbach, M. L., Cao, G., Williams, J. T., Finklestein, J. M., & Delisser, H. M. Isolation of murine lung endothelial cells. Am J Physiol Lung Cell Mol Physiol. **296**, L1096–L1103 (2009). https://www.ncbi.nlm.nih.gov/pubmed/19304908

37. Pukhalsky, A. L., Toptygina, A. P., and Viktorov, V. V. Pharmacokinetics of alkylating metabolites of cyclophosphamide in different strains of mice. Int J Immunopharmacol. **12**, 217-223 (1990). https://www.ncbi.nlm.nih.gov/pubmed/2329014
38. Hiratsuka, S., Goel, S., Kamoun, W.S., Maru, Y., Fukumura, D., Duda, D.G. & Jain, R.K. Endothelial focal adhesion kinase mediates cancer cell homing to discrete regions of the lungs via e-selectin up-regulation. Proc Natl Acad Sci USA. **108**, 3725-3730 (2011). https://www.ncbi.nlm.nih.gov/pubmed/21321210
39. Gakhar, G., Navarro, V. N., Jurish, M., Lee, G. Y., Tagawa, S. T., Akhtar, N. H., Seandel, M., Geng, Y., Liu, H., Bander, N. H., Giannakakou, P., Christos, P. J., King, M. R., Nanus, D. M. Circulating Tumor Cells from Prostate Cancer Patients Interact with E-Selectin under Physiologic Blood Flow. PLoS ONE. **8**, e85143 (2013). https://www.ncbi.nlm.nih.gov/pubmed/24386459
40. Ramis-Conde, I., Chaplain, M. A., Anderson, A. R., Drasdo, D. Multi-scale modelling of cancer cell intravasation: the role of cadherins in metastasis. Phys Biol. **6**, 016008 (2009). https://www.ncbi.nlm.nih.gov/pubmed/19321920
41. Mrozik, K. M., Blaschuk, O. W., Cheong, C. M., Zannettino, A., & Vandyke, K. N-cadherin in cancer metastasis, its emerging role in haematological malignancies and potential as a therapeutic target in cancer. BMC Cancer. **18**, 939 (2018). https://www.ncbi.nlm.nih.gov/pubmed/30285678
42. Qi, J., Chen, N., Wang, J., & Siu, C. H. Transendothelial migration of melanoma cells involves N-cadherin-mediated adhesion and activation of the beta-catenin signaling pathway. Mol Biol Cell. **16**, 4386–4397 (2005). https://www.ncbi.nlm.nih.gov/pubmed/15987741
43. Kim, J. Y., Jeong, H. S., Chung, T., Kim, M., Lee, J. H., Jung, W. H., & Koo, J. S. The value of phosphohistone H3 as a proliferation marker for evaluating invasive breast cancers: A comparative study with Ki67. Oncotarget. **8**, 65064–65076 (2017). https://www.ncbi.nlm.nih.gov/pmc/articles/PMC5630312/
44. Ahlmann, M. & Hempel, G. The effect of cyclophosphamide on the immune system: implication for clinical cancer therapy. Cancer Chemother Pharmacol. **78**, 661 (2016). https://www.ncbi.nlm.nih.gov/pubmed/27646791
45. Van Tilburg, C.M., van Gent, R., Bierings, M.B., Otto, S. A., Sanders, E. A. M., Nibbelke, E. E., Gaiser, J. F., Janssens-Korpela, P. L., Wolfs, T. F. W., Bloem, A. C., Borghans, J. A. M., Tesselaar, K. Immune reconstitution in children following chemotherapy for haematological malignancies: a long-term follow-up. Brit J Haematol. **152**, (2011). https://www.ncbi.nlm.nih.gov/pubmed/21114483
46. Carella, Angelo & Pollicardo, N & R Raffo, M & Podesta, M & Carlier, P & Valbonesi, M & Lercari, G & Vitale, V & Gallamini, A. Intensive conventional chemotherapy can lead to a precocious overshoot of cytogenetically normal blood stem cells (BSC) in chronic myeloid leukemia and acute lymphoblastic leukemia. Leukemia. **6 Suppl 4**. 120-3 (1992). https://www.ncbi.nlm.nih.gov/pubmed/1359202
47. Yáñez, A., Coetzee, S. G., Olsson, A., Muench, D. E., Berman, B. P., Hazelett, D. J., … Goodridge, H. S. Granulocyte-monocyte progenitors and monocyte-dendritic cell

progenitors independently produce functionally distinct monocytes. Immunity. **47**, 890–902 (2017). https://www.ncbi.nlm.nih.gov/pubmed/29166589
48. Mitchell, A. J., Roediger, B., Weninger, W. Monocyte homeostasis and the plasticity of inflammatory monocytes. Cell Imunol. **291**, 22-31 (2014). https://www.ncbi.nlm.nih.gov/pubmed/24962351
49. Clausen, B. E., Burkhardt, C., Reith, W., Renkawitz, R., Forster, I. Conditional gene targeting in macrophages and granulocytes using lysMcre mice. Transgenic Res. **8**, 265-277 (1999). https://www.ncbi.nlm.nih.gov/pubmed/10621974
50. Nelson, E. R., Li, S., Kennedy, M., Payne, S., Kilibarda, K., Groth, J., Bowie, M., Parilla-Castellar, E., de Ridder, G., Marcom, P. K., Lyes, M., Peterson, B. L., Cook, M., Pizzo, S. V., McDonnell, D. P., Bachelder, R. E. Chemotherapy enriches for an invasive triple-negative breast tumor cell subpopulation expressing a precursor form of N-cadherin on the cell surface. Oncotarget. **7**, 84030–84042 (2016). https://www.ncbi.nlm.nih.gov/pmc/articles/PMC5356642/
51. Ye M., Iwasaki H., Laiosa, C. V., Stadtfeld, M., Xie, H., Heck, S., Clausen, B., Akashi, K., Graf, T. Hematopoeitic stem cells expressing the myeloid lysozyme gene retain long-term, multilineage repopulation potential. Immunity. **19**, 689-699 (2003). https://www.ncbi.nlm.nih.gov/pubmed/14614856
52. Kim, M. H., Yang D., Kim, M., Kim S. Y., Kim D, Kang S. J. A late-lineage murine neutrophil precursor population exhibits dynamic changes during demand-adapted granulopoiesis. Sci Rep. **7**, 39804 (2017). https://www.ncbi.nlm.nih.gov/pubmed/28059162
53. Magid, R., Murphy, T. J., and Galis, Z. S. Expression of matrix metalloproteinase-9 in endothelial cells is differentially regulated by shear stress. Role of c-myc. J Biol Chem. **278**, 32994-9 (2003). https://www.ncbi.nlm.nih.gov/pubmed/12816956
54. Wang, L., Zhang, Z. G., Zhang, R. L., Gregg, S. R., Hozeska-Solgot, A., LeTourneau, Y., Wang, Y., Chopp, M. Matrix metalloproteinase 2 (MMP2) and MMP9 secreted by erythropoietin-activated endothelial cells promote neural progenitor cell migration. J Neurosci. **28**, 5996-6003, (2006). https://www.ncbi.nlm.nih.gov/pubmed/16738242
55. Alva, J. A., Zovein, A. C., Monvoisin, A., Murphy, T., Salazar, A., Harvey, N. L., Carmeliet, P., Iruela-Arispe, M. L. VE-cadherin-Cre-recombinase transgenic mouse: a tool for lineage analysis and gene deletion in endothelial cells. Dev Dyn. **235**, 759-67 (2006). https://www.ncbi.nlm.nih.gov/pubmed/16450386